MULTIPLE ENDMEMBER SPECTRAL MIXTURE ANALYSIS:

ENDMEMBER CHOICE IN AN ARID SHRUBLAND

William J. Okin [1]
Gregory S. Okin [2]
Dar A. Roberts[2]
Bruce Murray[1]

1. INTRODUCTION

As the Earth's human population increases and once-fertile areas become less so, human activities are bound to spread into areas that once were considered barren and unworkable, namely our planet's arid and semi-arid regions. Worldwide, this process already has begun. As a result, these fragile areas are being put under stresses that are leading to severe landscape damage and hence, a decrease in usefulness to humans. This process of "desertification" is already widespread, and although many people frequently consider desertification to be a problem unique to arid and semi-arid Africa, it is in fact occurring on all continents except Antarctica.

Remote monitoring using current or anticipated satellite remote sensing is the most time- and cost-efficient way to proceed with arid region monitoring in the future. Unfortunately, interpretation of remote sensing data from arid regions is particularly difficult. Three factors are thought to contribute to this. First, arid and semi-arid regions are often characterized by large soil background, in many cases swamping out the spectral contribution of plants (Escafadel and Huete, 1991; Huete and Jackson, 1988; Huete et al., 1985; Smith et al., 1990). Second, light rays reaching sensors from desert plants are often polluted by additional interactions with desert soils (Huete, 1988; Ray and Murray, 1996). Finally, due to evolutionary adaptations to the harsh desert environment, desert plants are spectrally dissimilar to their humid counterparts, lacking in many cases a strong red edge, exhibiting reduced leaf absorption in the visible, and displaying strong wax absorptions around 1720 nm (Billings and Morris, 1951; Ehleringer, 1981; Ehleringer and Björkman, 1978; Gates et al., 1965; Mooney et al., 1977; Ray, 1995).

Many of the early applications of remote sensing to arid and semi-arid regions suggest that present remote sensing techniques, including most brightness and greenness indices, are susceptible to over- or underestimation of vegetation cover simply due to variations in soil color and low vegetation cover (Escafadel and Huete, 1991; Huete and Jackson, 1987; Huete and Jackson, 1988; Huete et al., 1985; Pickup et al., 1993) although Musick (1984) found a correlation between total vegetation cover and Landsat MSS band 5 brightness. None of theses studies were able to accurately and reliably discern shrubs from grasses in arid and semi-arid environments, which is probably the most important means by which to identify desertification in semi-arid grasslands (Schlesinger et al., 1990; Warren and Hutchinson, 1984). Later work by Franklin *et al*. (1993) and Duncan *et al*. (1993) using SPOT wavebands and greenness and brightness indices found these indices to be sensitive to vegetation type as well as cover. High variance in these studies, however, suggests that even in cases where landscape components were determined to be significantly different, it may not be possible to accurately retrieve the contribution of these components to spatially averaged reflectance measurements. This characteristic is presumably due to the low spectral resolution of the SPOT wavebands and the effect of nonlinear mixing under low cover conditions, as well as the typically high spectral variability found in desert plants.

Despite the lackluster performance of remote sensing in arid regions, there are have been a few studies that suggest there is potential for doing accurate and reliable remote sensing in arid and semi-arid regions. Smith *et al*. (1990) applied a mixing model that employed laboratory and field spectra to Landsat TM data from the Owens Valley, indicating that mixture modeling can facilitate mapping and monitoring of sparse vegetation cover. Roberts *et al*. (1997; 1993) have used linear mixture analysis of AVIRIS data to map green vegetation, nonphotosynthetic vegetation (NPV), and soils at the Jasper Ridge Biological Preserve and the Santa Monica Mountains, CA. It is a natural next step, therefore, to apply spectral mixture analysis to arid and semi-arid regions in the hope that this will

[1] Department of Geography, University of California, Santa Barbara, CA 93106
[2] Division of Geological and Planetary Sciences, 170-25,California Institute of Technology, Pasadena, CA, 91125

overcome previous difficulties in accurate and reliable landscape assessment by remote sensing in these areas. The purpose of this study is to determine if multiple endmember spectral mixture analysis will accurately and reliably characterize arid and semi-arid region vegetation and soils from AVIRIS data. The ultimate goal of this work is to develop tools for remote sensing of arid regions that make the best use of current and near-future remote sensing technology to monitor these environments.

2. METHOD

2.1 Study Site Description

The Manix Basin is in the Mojave Desert, about 25 miles ENE of Barstow in southeastern California (centered around 34°56.5" W 116°41.5" at an elevation of about 540 m). The basin was the site of ancient Lake Manix which existed during the peak pluvial episode of the last glaciation and drained about 14,000 yr. B.P. through Afton Canyon to the east; several smaller short-lived lakes followed this episode (Buwalda, 1914; Dohrenwend et al., 1991; Enzel et al., 1992; Meek, 1987; Morrison, 1991). Much of the basin is filled with fine- to medium-grained lacustrine, fluvial, and deltaic sediments capped by weak deflational armoring consisting of gravel-sized particles concentrated at the soil surface (Buwalda, 1914; Dohrenwend et al., 1991; Meek, 1990). There is clear evidence of pre-modern aeolian sand mobilization (Dohrenwend et al., 1991; Evans, 1992; Meek, 1990; Sharp, 1966), indicating that wind erosion has a long history as a geological process in the area. At present, two playas exist within the Manix Basin: Coyote Dry Lake and Troy Dry Lake.

The modern climate of the Manix Basin is essentially Mediterranean with precipitation falling mostly in the winter, although there is significant summer monsoonal precipitation in some years (National Climate Data Center, 1993). The average annual temperature is 19.6°C, the average winter temperature is 9.1°C, and the average summer temperature is 31.4°C. (Meek, 1990) The average wind speed at the airport in Daggett is greater than 5 m/s at a height of 6.1 m (National Climate Data Center, 1993).

The vegetation in undisturbed areas of the basin is dominated by an association of *Larrea tridentata* (Creosote bush) and *Ambrosia dumosa* (White Bursage or Burro Bush) with minor occurrence of *Atriplex polycarpa* (Desert Saltbush), *Atriplex hymenelytra* (Desert Holly), *Atriplex canescens* (Four-Winged Saltbush), *Ephedra* (Mormon Tea), and *Opuntia* (Cholla). *Prosopis glandulosa* (Mesquite) occurs in the western portion of the basin. A species of *Schismus* is the dominant annual grass in the basin, and can have high cover in years of high winter/spring precipitation.

There has been extensive human activity in the Manix Basin, with several phases of agricultural activity, made possible by annual groundwater recharge from the Mojave River which carries runoff from the San Bernardino Mountains to the south-southwest (Tugel and Woodruff, 1978). Establishment and subsequent abandonment of agricultural lands in the Manix Basin has been associated with indirect disturbance of adjacent, downwind areas by sand blown off of the areas of direct disturbance (Okin et al., In Preparation; Ray, 1995). This has led to decreased shrub density, increased soil albedo, and changes in soil texture in these areas. The abandoned fields themselves are either dominated by *Atriplex polycarpa* with total cover often greater than that in undisturbed desert, or bare of perennial shrub cover. There are housing developments in the basin, many of which are situated around a central reservoir. Roads and off-road vehicle tracks are ubiquitous.

2.2 Image Acquisition and Processing

AVIRIS data were acquired over the Manix Basin on April 30, 1998. After they were acquired, the data were radiometrically corrected at the AVIRIS data facility. Apparent surface reflectance was retrieved using a technique developed by Green *et al*. (Green et al., 1993; Green et al., 1996; Roberts et al., 1998; Roberts et al., 1997). The reflectance spectrum from a gravel parking lot in the AVIRIS scene was used to calibrate the apparent surface reflectance spectra of the entire scene.

2.3 Multiple Endmember Spectral Mixture Analysis

Spectral mixture analysis (SMA) is based on the assumption that the reflectance spectrum derived from an air- or spaceborne sensor can be deconvolved into a linear mixture of the spectra of ground components, frequently

called spectral endmembers. The best-fit weighting coefficients of each ground component spectrum, which must sum to one, are interpreted as the relative area occupied by each component in a pixel. Multiple endmember spectral mixture analysis (MESMA) is simply a SMA approach in which many possible mixture models are analyzed in order to produce the best fit (Gardner, 1997; Painter et al., 1998; Roberts et al., 1998). In the MESMA approach, a "spectral library" is defined which contains spectra, convolved to the 224 AVIRIS bands, of plausible ground components. A set of mixture models with n ($n \geq 2$) endmembers from the library is defined, with photogrammetric shade always present as one endmember in the model. The weighting coefficients (fractions) for each model and each pixel are determined such that the linear combination of the endmember spectra produces the lowest RMS error when compared to the apparent surface reflectance for the pixel. Weighting coefficients are constrained to be between zero and one, and a valid fit is restricted to a maximum preset RMS error. Models that meet these constraints are recorded, which typically yields several possible models for each pixel. As an optional final step, one representative model can be identified for each pixel, which requires choosing both the appropriate number of endmembers of each pixel, and the optimal model which has the appropriate number of endmembers. It is these best-fit models and the methodology for choosing them that are discussed below.

This approach requires an extensive library of field, laboratory, and image spectra, where each plausible ground component is represented at least once. Including more than one spectrum of a ground component allows for the considerable spectral variability often found in desert vegetation, thus overcoming a difficulty identified by Franklin *et al*. (1993) of doing remote sensing in arid regions.

2.4 Methods Used in This Study

In this study two-, three-, and four-endmember models were analyzed using the apparent surface reflectance retrieval from an AVIRIS scene which includes the northern lobe of the Manix Basin (flight 980430 run 10 scene 3). Field spectra collected in the Manix Basin on May 2, 1998 were incorporated into the spectral library in this study in order to make as direct an identification of landscape components as possible. Spectra of soils from other dates were used to supplement this library. Field spectra were collected from 350 nm to 2500 nm using an ASD Full Range portable spectroradiometer (Analytical Spectral Devices, Inc., Boulder, CO) on loan from the Jet Propulsion Laboratory. With a 100% reflective Spectralon panel, spectra can be displayed and recorded in real-time as reflectance.

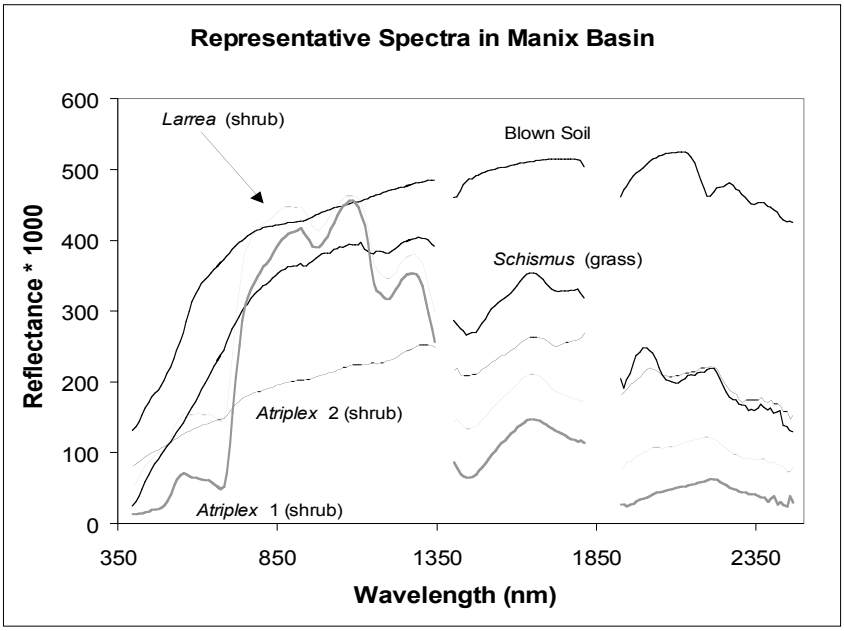

Figure 1. Representative spectra in the Manix Basin spectral library

A total of 68 field spectra were chosen to be included in the spectral library for this study. This includes 12 grass and NPV spectra, 42 shrub spectra and 14 soil spectra. Representative spectra are shown in Figure 1. For our

analysis, soil spectra were divided into three groups: armored soils, soils from abandoned fields, and blown sand. The blown sand is spectrally bright, and has much smaller surface particle size than the other two soils. The soils from the abandoned fields, although disturbed, are characterized by a weak deflationary crust of pebble size clasts, while the armored soils have a stronger deflationary armor with larger clasts, and are indicative of thousands of years of undisturbed development. The grass category consists of herbaceous annuals and *Schismus* grass which were by and large senesced by the image acquisition date. Shrubs were categorized by genus. In Figure 1, the fact that *Atriplex* 1 looks less like another shrub of the same genus (*Atriplex* 2) than like a shrub of a different genus (*Larrea*) illustrates the difficulty of differentiating arid shrub taxa from one another spectrally. Spectra used in four-endmember models were chosen to minimize computation time and to maximize spectral variability using the method outlined by Gardner (1997) and Roberts *et al*. (1998). In this library analysis, each spectrum in the spectral library is modeled by every other spectrum in the library, coupled with shade, and constrained by the constraints that will be used in the final analysis. This approach allows spectra to be compared to one another, and redundant or unique spectra to be identified. Spectra were chosen that 1) modeled other spectra of the same type, 2) were not modeled by other spectra of the same type, and 3) were not confused with spectra of other types.

For the two-endmember models, the entire spectral library was used in MESMA modeling, resulting in 68 models. For the three-endmember models, all soil + grass + shade, soil + shrub + shade, grass + shrub + shade combinations from a slightly reduced library (13 soils, 42 shrubs, 11 grasses) were used, resulting in a total of 1,175 different models. Finally, for the four-endmember models, nine soil spectra, eight grass spectra, and nineteen shrub spectra were used to define a total of 2,907 soil + grass + shrub + shade and soil + shrub + shrub + shade models. The models with two shrubs and no grasses were included because when shrubs dominate an area in the Manix Basin, it is often a mixture of at least two species.

A total of 4,141 models were considered in this analysis. The advantage of using many possible mixture models for each pixel comes at the cost of increased computational effort. In order to address the computational requirements of considering thousands of models for each pixel, we used a parallel-processing computer, the HP Exemplar X-Class System, jointly owned by Caltech and JPL. With 256 processors and 64GB of memory, the Exemplar allows many lines of an image to be processed simultaneously, greatly reducing the computation time over a sequentially processed image. All of the three and four endmember models were processed on this machine. The minimum RMS threshold was set at 2.5% for all 4,141 models.

With many models to choose from for each pixel, the choice of the most representative model for each pixel becomes difficult. When dealing with a fixed number of endmembers, it is reasonable to choose the model with the lowest error. However, when comparing models of a variable number of endmembers the RMS is not an appropriate metric, since increasing the degrees of freedom by adding additional endmembers will always reduce the error. Thus, if all of the same spectra are used, the lowest error four-endmember model should always have lower error than the lowest error three-endmember model.

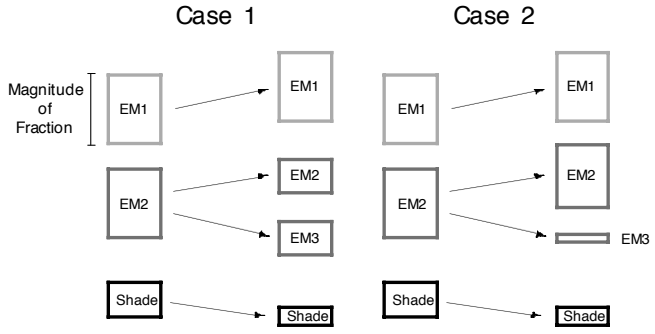

Figure 2. Consequences of adding a fourth endmember

Other ways of comparing between models of different degree include the consideration of a dramatic reduction in RMS, the categorical changes in endmembers that might take place when changing the number of endmembers, and the relative magnitude of the fractions in models of different degree. This last approach was used in this analysis. Figure 2 illustrates two possible cases when three- and four-endmember results are being compared.

In Case 1, the added flexibility of a fourth endmember allows the second endmember in the three-endmember case to be split into two separate endmembers that significantly contribute to the mixture. An example of this is the situation where both shrubs and grasses exist in a pixel, but in a three-endmember model only one vegetation endmember is allowed in addition to soil and shade, so either a grass or a shrub must be used. The four-endmember model allows both a shrub and a grass to contribute to the mixture, more accurately representing the actual contents of the pixel. In Case 2, a fourth endmember is allowed, but the magnitude of its fraction is very small. Here it is impossible to tell if the added endmember is modeling something that exists in the pixel, or if it is being added marginally to improve the fit of inadequate endmember spectra in a more or less three-endmember pixel. It is parsimonious to exclude this fourth endmember if its fraction is small enough, because it is difficult to defend the significance of its contribution to understanding the contents of the pixel. In our analysis, this case was identified by setting a minimum threshold for acceptable non-shade fractions.

3. RESULTS AND DISCUSSION

Figure 3a is a false color composite of the reflectance image of the Manix Basin, where red is 1580nm, green is 830nm and blue is 650nm. This image has several easily identifiable features which will be used in the subsequent discussion of our results using MESMA. There are four abandoned fields labeled on the image, for which the general distribution of vegetation is known. Fields one and two have significant shrub cover, while fields three and four are exclusively grass covered. Several areas of mobile soil can be identified. The northern part of the image, or lower right of the plate, has obvious dune features, which are primarily sand. The prevailing wind direction in the basin is west to east, and plumes of sandy soils can be seen extending in the downwind direction from fields one, three and four as well as other disturbed areas in the western part of the image. The toes of alluvial fans are evident on southwest and northeast edges of the image, which have higher shrub cover in general than the basin floor. The north edge of the image is the edge of Coyote Dry Lake, and due to the perennial nature of the lake here, this area has very little vegetation.

3.1 Two-Endmember Models

Two endmembers modeled less than 11% of the image, and all of these models contained a soil endmember in addition to shade. The modeled areas are exclusively in the northern corner and northeastern edge of the image, on Coyote Playa and an alluvial fan. While the playa is mostly barren of vegetation, the alluvial fan has some shrub coverage. Besides the playa margin, there are almost no pure soil pixels in the basin. The fact that the only feasible two-endmember models were soils implies that the first-order signal in the image is soil, which is to be expected in an arid environment and indeed confirms other authors' results that soil is the major spectral contributor to remote sensing data in arid and semi-arid regions (Huete *et al.*, 1985; Huete and Jackson, 1988; Smith *et al*., 1990; Escafadel and Huete, 1991). This result also suggests that since the soil signal is so strong, every model should include a soil endmember.

3.2 Three-Endmember Models

The three-endmember models were divided into three categories: soil + shrub + shade, soil + grass + shade, and shrub + grass + shade. Using only three endmembers, 98.6% of the image was modeled. The lowest RMS model for each pixel nearly always contained a soil endmember, again illustrating the strength of the soil signal. Figure 3b shows the vegetation endmember chosen for each pixel, indicating that most of the basin was modeled by grass and soil. Fields three and four are correctly modeled as grasses. While grasses were widespread in 1998 due to the El Niño precipitation, shrubs are also widespread in the basin. Clearly, in some cases the shrubs are being underrepresented by the three endmember results. Shrubs are modeled on the alluvial fans, which is reasonable, but the shrubs in fields one and two are being missed entirely. The soil category chosen for each pixel is illustrated in Figure 3c. The dune area in the north is correctly modeled with the sandy blown soil endmembers, as are the two short plumes coming off of fields three and four. However, the disturbed southern and eastern part of the image, the large plume off of field one, and several abandoned fields are modeled predominantly by the armored soils. These results are not reasonable because the armored soils are indicative of thousands of years of stability. Field observations clearly indicate that these soils are not armored.

Thus, given the 2.5% RMS constraint, three endmembers are able to model most of the image. While in some cases this seems to do reasonably well, there are other cases where three endmembers are probably not enough

to capture the variability within a pixel. Further, there are a few bare regions, such as the playa margin, which probably don't need a vegetation endmember.

3.3 Four-Endmember Models

In this arid region of California, there are two basic vegetation types: shrubs and grasses. Since the two- and three-endmember modes have shown that soil is the dominant signal in the image, a soil endmember must be included in any spectral mixture model in this region. Thus, to capture the two vegetation types, four endmembers will often be needed: soil, shrub, grass, and shade. In areas where shrubs dominate, it is unlikely that all the shrubs in a pixel will be spectrally similar, given the spectral variability of shrubs both between and within the genus categories. Four endmembers allows models that may capture this variability by including two different shrubs, a soil, and shade.

With the 2.5% RMS constraint, the 2,907 four-endmember models defined fit 98.1% of the image. This is slightly reduced from the three-endmember case because several of the library spectra had to be omitted in the four-endmember case to keep the number of models reasonable, even for computation on a supercomputer. *Larrea* and *Atriplex* were the two shrub categories picked predominantly, which agrees with the general distribution of shrub genera in the basin. The models with two shrub endmembers accounted for only 8.2% of the entire image, indicating that including a grass and a shrub endmember is much more valuable than having two shrubs. Figure 3d is a false color composite where red is the soil fraction, green is the first shrub fraction, and blue is the grass or second shrub fraction. Grass still arises as the dominant vegetation type throughout the basin, but shrubs are much more widely represented than in previous cases. Where the three-endmember case misrepresented the shrubs known to exist in fields one and two, the four-endmember case clearly picks up the shrubs in those fields, while still accurately modeling fields three and four as mostly grass. The western fan also shows more shrub cover than with three endmembers while the eastern fan and the playa margin are consistently dominated by soil, with small amounts of shrubs, and virtually no grasses.

The soil category for the best four-endmember model in each pixel is shown in Figure 3e. As with the three-endmember case, the dunes in the north model mostly as sandy soil. The large plumes east of field one, and the disturbed eastern part of the image is dominated by the sandy soil which makes sense given the prevailing wind direction and the evidence of agriculture upwind. However, some clearly disturbed areas, such as field one and other fields still erroneously model as armored soil, indicating perhaps that a gap exists in the soil spectra in the spectral library.

The flexibility of four endmembers allows some deficiencies in the three-endmember results to be remedied. However, there are some instances where four endmembers clearly overfit the environment. Since none of the cases where the number of endmembers is constant across the entire image is obviously superior, a method to integrate these cases into one result is needed.

3.4 Choosing the Appropriate Number of Endmembers for Each Pixel

A pixel that is overfit can be expected to have at least one fraction that is significantly lower than the others (Figure 2). Ideally, an unnecessary endmember would have a zero fraction, but given the spectral variability of components in the environment, and a limited spectral library, this perfect fit will only rarely occur. Figure 4 contains a histogram of the minimum non-shade fraction of the optimal three- and four-endmember models across the entire image. The minimum four-endmember fraction is always quite small, most of them less than 7%, indicating that many of these pixels may be overfit. The histogram for three endmembers is bimodal, with one maximum at about 32% and the other maximum at about 5%. This implies that many pixels modeled with three endmembers have two non-shade endmembers of significant magnitude, but in some cases there is a fraction so small that the third endmember may be superfluous.

A minimum fraction threshold was set at 5% to identify fractions deemed insignificant. Using this threshold, the lowest RMS two-, three- and four-endmember models were compared for each pixel. The model with the highest number of endmembers whose non-shade fractions were all at least 5% was chosen for each pixel to produce an integrated result. Figure 5a shows the distribution of the final number of endmembers chosen by this method. Four endmembers were used to model 41.1% of the image and occur in most of the southern part of the

image, particularly the areas downwind of the abandoned fields, the western fan, and the much of the dune area. Three endmembers account for 54.7% of the image and prevail in the undisturbed western part of the image, the eastern fan, and the edge of Coyote Dry Lake. Only in a few pixels (1.7%) are two endmembers favorable over three. Figure 5b shows the composition of the vegetation fraction (three-endmember case) or fractions (four-endmember case). Fields one and two and both fans retain significant shrub fractions, while grass is prevalent across much of the basin. The disturbed areas east of the fields show a significant mixture of shrubs and grasses. Figure 5c shows the soil category for the integrated results, which is virtually identical to the soils from the four-endmember case.

While more than half of the image can be well modeled with three endmembers, the four endmember case allows much greater flexibility in the vegetation fraction, which affects not only the interpretation of the vegetation, but the interpretation of the soil as well. Elsewhere, we have shown that a deficiency in the vegetation endmembers can force an erroneous soil to be in the optimal model (Okin *et al.*, 1997). As a result, the option of including two vegetation endmembers when appropriate not only represents the vegetation more accurately, but also gives us more confidence in the soil endmember choice. Thus, the ability to combine two-, three-, and four-endmember model results into a single image using a simple selection criterion greatly enhances our ability to correctly identify ground constituents.

4. CONCLUSIONS

It was the purpose of this study to determine if the MESMA approach can provide an accurate and reliable means to characterize arid and semi-arid region vegetation and soils from AVIRIS data. The results presented here indicate that MESMA can successfully capture some of the most important landscape features that are relevant for desertification monitoring, such as shrub and grass distributions. Furthermore, since the soil signal is so strong in dry regions, AVIRIS combined with MESMA can provide spatially distributed information on soil surface characteristics that may greatly aid in the mapping of soils. Two-endmember models are inadequate for mixture modeling of arid and semi-arid environments except in extreme, and rare, cases of bare soil. Application of three-endmember models indicates that these models might be adequate in many areas, but do not have the flexibility to characterize a complex arid or semi-arid landscape that has two distinct vegetation types. Four-endmember models provide enough flexibility to account for some of the complexity of this arid environment, but may not be appropriate everywhere.

A method was devised to integrate two-, three-, and four-endmember models into a final result by eliminating higher order models which had small non-shade fractions. Allowing the number of endmembers to vary across the scene allows us to more accurately model the variation on the landscape. While these integrated results resemble the four-endmember case more than the three-endmember case, the areas where fewer endmembers are necessary are indicative of regions with less complex variation in vegetation types. Undisturbed areas of the Manix Basin are modeled better by grasses than shrubs or a combination of shrubs and grasses. Shrubs are perennial features of the undisturbed desert and are ubiquitous in the undisturbed, non-playa-margin areas of the basin. Nonetheless, they can have low fractional cover compared to grasses, especially in this scene from a very wet El Niño year. The overall high abundance of grass compared to shrubs in this scene is largely a result of interannual variability caused by short-term climate fluctuations. In other years, grasses can be expected to be largely absent. Nonetheless, the final results do highlight areas of direct or indirect disturbance quite well by indicating areas of blown sand, by indicating that some old fields are covered with shrubs, and finally by indicating that areas downwind of abandoned fields have less grass than areas in the undisturbed desert.

5. FUTURE RESEARCH

In complex arid and semi-arid environments, the number of components that exist in a given pixel can vary, so it is essential that methods to model these environments take this variability into account. We have presented one possible way to choose between variable numbers of endmembers from a MESMA analysis. There are other approaches, such as taking into consideration the attributes of the endmembers, a large reduction in RMS, and spatial continuity which may be fruitful in future research. The method we have presented would benefit from sensitivity analysis with respect to the minimum fraction threshold. Finally, a well-planned field campaign to verify the results in the Manix Basin and to broaden the spectral library will allow us to better evaluate the performance of

MESMA and AVIRIS as tools to characterize the Mojave Desert in particular, and arid and semi-arid environments in general.

6. REFERENCES

Billings, W.D., and Morris, R.J., 1951, Reflection of visible and infrared radiation for leaves of different ecological groups: American Journal of Botany, v. 39, p. 327-331.

Buwalda, J.P., 1914, Pleistocene beds at Manix in the eastern Mohave Desert region: University of California Bulletin of the Department of Geology, v. 7, p. 443-464.

Dohrenwend, J.C., Bull, W.B., McFadden, L.D., Smith, G.I., Smithe, R.S.U., and Wells, S.G., 1991, Quaternary geology of the Basin and Range province in California, *in* Morrison, R.B., ed., Quaternary Nonglacial Geology: Coterminous U.S., Volume K-2: Boulder, Colorado, Geological Society of America, p. 321-352.

Duncan, J., Stow, D., Franklin, J., and Hope, A., 1993, Assessing the relationship between spectral vegetation indices and shrub cover in the Jornada Basin, New Mexico: International Journal of Remote Sensing, v. 14, p. 3395-3416.

Ehleringer, J., 1981, Leaf absorptances of Mohave and Sonoran Desert plants: Oecologia, v. 49, p. 366-370.

Ehleringer, J.R., and Björkman, O., 1978, Pubescence and leaf spectral characteristics in a desert shrub, *Encilia farinosa*: Oecologia, v. 36, p. 151-162.

Enzel, Y., Brown, W.J., Anderson, R.Y., McFadden, L.D., and Wells, S.G., 1992, Short-duration Holocene lakes in the Mojave River drainage basin, Southern California: Quaternary Research, v. 38, p. 60-73.

Escafadel, R., and Huete, A.R., 1991, Improvement in remote sensing of low vegetation cover in arid regions by correcting vegetation indices for soil "noise": C. R. Academie des Sciences Paris, v. 312, p. 1385-1391.

Evans, J.R., 1992, Falling and climbing sand dunes in the Cronese ("Cat") Mountain Area, San Bernardino County, California: California Division of Mines, Geological Notes, p. 107-113.

Franklin, J., Duncan, J., and Turner, D.L., 1993, Reflectance of vegetation and soil in Chihuahuan desert plant communities from ground radiometry using SPOT wavebands: Remote Sensing of the Environment, v. 46, p. 291-304.

Gardner, M., 1997, Mapping Chaparral with AVIRIS Using Advanced Remote Sensing Techniques [Master of Arts thesis]: Santa Barbara, CA, University of California, CA.

Gates, D.M., Keegan, H.J., Schleter, J.C., and Weidner, V.R., 1965, Spectral Properties of Plants: Applied Optics, v. 4, p. 11-20.

Green, R.O., Conel, J.E., and Roberts, D.A., 1993, Estimation of aerosol optical depth and additional atmospheric parameters for the calculation of apparent surface reflectance from radiance measured by the Airborne Visible/Infrared Imaging Spectrometer, *in* Green, R.O., ed., Fourth Annual JPL Airborne Geoscience Workshop, Volume 1: Pasadena, CA, Jet Propulsion Laboratory, p. 73-76.

Green, R.O., Roberts, D.A., and Conel, J.E., 1996, Characterization and compensation of the atmosphere for the inversion of AVIRIS calibrated radiance to apparent surface reflectance, *in* Green, R.O., ed., Sixth Annual JPL Airborne Earth Science Workshop, Volume 1: Pasadena, CA, Jet Propulsion Laboratory, p. 135-146.

Huete, A.R., 1988, A soil-adjusted vegetation index (SAVI): Remote Sensing of Environment, v. 25, p. 295-309.

Huete, A.R., and Jackson, R.D., 1987, Suitability of spectral indices for evaluating vegetation characteristics on arid rangelands: Remote Sensing of the Environment, v. 23, p. 213-232.

Huete, A.R., and Jackson, R.D., 1988, Soil and atmosphere influences on the spectra of partial canopies: Remote Sensing of Environment, v. 25, p. 89-105.

Huete, A.R., Jackson, R.D., and Post, D.F., 1985, Spectral response of a plant canopy with different soil backgrounds: Remote Sensing of Environment, v. 17, p. 37-53.

Meek, N., 1987, Geomorphic and hydrologic implications of the rapid incision of Afton Canyon, Mojave Desert, California: Geology, v. 17, p. 7-10.

Meek, N., 1990, Late Quaternary Geochronology and Geomorphology of the Manix Basin, San Bernardino County, California [Ph.D. thesis]: Los Angeles, California, University of California at Los Angeles.

Mooney, H.A., Ehleringer, J., and Björkman, O., 1977, The energy balance of leaves of the evergreen desert shrub *Atriplex hymenelytra*: Oecologia, v. 29, p. 301-310.

Morrison, R.B., 1991, Quaternary geology of the southern Basin and Range Province, *in* Morrison, R.B., ed., Quaternary Nonglacial Geology: Coterminous U.S., Volume K-2: Boulder, Colorado, Geological Society of America.

Musick, H.B., 1984, Assessment of Landsat Multispectral Scanner spectral indices for monitoring arid rangeland: IEEE Transactions on Geoscience and Remote Sensing, v. GE-22, p. 512-519.

National Climate Data Center, 1993, Solar and Meteorological Surface Observation Network: 1961-1990, Volume III: Western United States, National Climate Data Center.

Okin, G.S., Schlesinger, W.H., and Murray, B., In Preparation, Desert shrubland degradation: Physical and biogeochemical feedbacks: .

Painter, T.H., Roberts, D.A., Green, R.O., and Dozier, J., 1998, The effect of grain size on spectral mixture analysis of show-covered area from AVIIRS data: Remote Sensing of Environment, v. 65, p. 320-332.

Pickup, G., Chewings, V.H., and Nelson, D.J., 1993, Estimating changes in vegetation cover over time in arid rangelands using Landsat MSS data: Remote Sensing of Environment, v. 43, p. 243-263.

Ray, T.W., 1995, Remote Monitoring of Land Degradation in Arid/Semiarid Regions [Ph.D. thesis]: Pasadena, CA, California Institute of Technology.

Ray, T.W., and Murray, B.C., 1996, Nonlinear spectral mixing in desert vegetation: Remote Sensing of Environment, v. 55, p. 59-64.

Roberts, D.A., Gardner, M., Church, R., Ustin, S., Scheer, G., and Green, R.O., 1998, Mapping chaparral in the Santa Monica Mountains using multiple endmember spectral mixture models: Remote Sensing of Environment, v. 65, p. 267-279.

Roberts, D.A., Green, R.O., and Adams, J.B., 1997, Temporal and spatial patterns in vegetation and atmospheric properties from AVIRIS: Remote Sensing of Environment, v. 62, p. 223-240.

Roberts, D.A., Smith, M.O., and Adams, J.B., 1993, Green vegetation, nonphotosynthetic vegetation, and soils in AVIRIS data: Remote Sensing of the Environment, v. 44, p. 255-269.

Schlesinger, W.H., Reynolds, J.F., Cunningham, G.L., Huenneke, L.F., Jarrell, W.M., Virginia, R.A., and Whitford, W.G., 1990, Biological Feedbacks in Global Desertification: Science, v. 247, p. 1043-1048.

Sharp, R.P., 1966, Kelso Dunes, Mojave Desert, California: Geological Society of America Bulletin, v. 77, p. 1045-1074.

Smith, M.O., Ustin, S.L., Adams, J.B., and Gillespie, A.R., 1990, Vegetation in deserts: I. a regional measure of abundance from multispectral images: Remote Sensing of the Environment, v. 31, p. 1-26.

Tugel, A.J., and Woodruff, G.A., 1978, Soil Survey of San Bernardino County, California: Mojave River Area: Washington, D. C., Soil Conservation Service, United States Department of Agriculture.

Warren, P.L., and Hutchinson, C.F., 1984, Indicators of rangeland change and their potential for remote sensing: Journal of Arid Environments, v. 7, p. 107-126.